

# Static and dynamic properties of hydrogenated amorphous silicon with voids

S. Chakraborty

Department of Physics and Astronomy, Ohio University, Athens, Ohio 45701, USA

D. A. Drabold

Trinity College, Cambridge CB2 1TQ, United Kingdom

and Department of Physics and Astronomy, Ohio University, Athens, Ohio 45701, USA

(Received 15 December 2008; revised manuscript received 9 February 2009; published 30 March 2009)

We have employed *ab initio* techniques to study the structure and dynamics of voids in amorphous Si and hydrogenated amorphous silicon. Reconstruction effects at void surfaces and dynamical effects associated with H are particularly emphasized. We introduce unbonded H into the network, track its diffusive motion, and note a strong tendency for H to attack strained structures in the network. We compare our models to recent NMR experiments. Consistent with these experiments, our results are indicative of a mean proton-proton separation of  $1.8 \pm 0.2$  Å, and identify the probable bonding configurations of clustered hydrogen in a divacancy giving rise to this separation. We also discuss the role of voids and hydrogen motion on the electronic structure.

DOI: [10.1103/PhysRevB.79.115214](https://doi.org/10.1103/PhysRevB.79.115214)

PACS number(s): 61.43.Bn, 71.15.Pd, 71.23.-k

## I. INTRODUCTION

Hydrogenated amorphous silicon (*a*-Si:H) is a technologically important material, used extensively in solar photovoltaics, thin-film transistor, and IR detection/imaging applications. The accepted structural model for (unhydrogenated) *a*-Si is the continuous random network. These models are satisfactory for many problems and have been a great help in unraveling questions of electronic structure,<sup>1,2</sup> electronic transport,<sup>3</sup> and thermal transport.<sup>4</sup> Upon closer inspection, however, it is clear that many thin films of *a*-Si:H are heterogeneous and may include paracrystals<sup>5</sup> and microvoids.<sup>6</sup> Our aim in this paper is to use current *ab initio* techniques to determine static and dynamical properties of the voids. Probably the most interesting feature of our work is the interplay between voids, strained bonds or rings and dynamic H. As we have reported elsewhere,<sup>7</sup> H is more mobile than previously believed and hops in ways unanticipated from experience of H in crystalline Si. Because H selectively attacks distorted parts of the network, voids (or indeed grain boundaries) play an important role in the motion of H.<sup>8</sup>

The presence of voids in *a*-Si:H has been documented by small angle x-ray scattering studies.<sup>9,10</sup> Early nuclear magnetic resonance (NMR) experiments on PECVD films showed that H occupies both isolated and clustered environments with a small fraction of H<sub>2</sub> molecules existing in larger voids.<sup>11</sup> Further, multiple quantum NMR studies on plasma enhanced chemical vapor deposition (PECVD) films showed evidence of clusters of six hydrogen atoms in divacancy-(DV-) like voids.<sup>12</sup> Recent studies by Longeaud<sup>13</sup> have linked H<sub>2</sub> trapped in the voids in *a*-Si:H with metastability. Although the existence of H<sub>2</sub> in *a*-Si:H has been reported by Beyer<sup>14</sup> and Roura *et al.*,<sup>15</sup> the identity of formation sites of H<sub>2</sub> within the network is still uncertain. Our work is motivated particularly by the proton NMR studies of Bobela *et al.*,<sup>16</sup> who interpret their data to be a consequence of dipolar-coupled H pairs separated, on average, by  $1.8 \pm 0.1$  Å. Our work supports this view and we provide additional information about the relevant structures.

Finally, our work is salient to studies of *a*-Si and *a*-Si:H

surfaces<sup>17</sup> (in this case they are of course *internal* surfaces). Perhaps unsurprisingly, we find that reconstruction effects for *a*-Si can be understood to a significant degree in terms of the system rearranging itself to minimize dangling bonds. The case of *a*-Si:H turns out to be of much more interest because of the important role of H passivation of strained or defective sites, and especially the role of H dynamics in this large and highly heterogeneous system.

The greatest shortcoming of this paper is that statistics are limited. We are able to provide a highly detailed glimpse of important physical processes, but because of computational expense cannot make an extensive list of events and their probabilities. Nevertheless, we believe that the content of this paper is a strong complement to experimental work which has almost the opposite deficiencies—there is no trouble extracting long-time behavior, but it is difficult to extract dynamical processes on the atomistic level from experiments.

The rest of the paper is organized as follows. In Sec. II, we discuss the details of the density-functional code used, details of the Hamiltonian employed, and the nature of the models that we begin with. In Sec. III, we describe the structural characteristics of voids and focus on the salience of these calculations to NMR experiments. Section IV is concerned with H dynamics in models with voids, and Sec. V reveals electronic signatures of voids.

## II. METHODOLOGY AND MODELS

In our simulations, we used SIESTA, a density-functional theory based first-principles local orbital code.<sup>18–20</sup> SIESTA uses norm-conserving Troullier-Martins pseudopotentials<sup>21</sup> in factorized Kleinman-Bylander<sup>22</sup> form. Here, we use the generalized gradient approximation of Perdew, Burke and Ernzerhof.<sup>23</sup> As the energetics of H is delicate,<sup>24,25</sup> high quality approximations are required. Double-zeta polarized basis sets for silicon and hydrogen are used (two *s* and three *p* orbitals for the H valence electrons, and two *s*, six *p*, and five *d* orbitals for Si valence electrons). To independently check

our approximations, we have repeated our calculations using the plane-wave code VASP.<sup>26</sup> Our results with SIESTA are essentially identical to the results from VASP.

We studied configurations of *a*-Si:H with various concentrations of H and different void sizes. We began with two well-relaxed defect-free CRN models of amorphous silicon of 216 atoms and 64 atoms due to Barkema and Mousseau,<sup>27</sup> obtained with an improved Wooten Winer and Weaire (WWW)<sup>28</sup> bond-switching method. A model of *a*-Si:H with a DV is created by removing two Si atoms that are nearest neighbors, then terminating the resulting dangling Si bonds with H. To begin to explore the role of site dependence, we generated four DV models (with randomly chosen starting sites) for both the large and small models. Models of *a*-Si:H with larger voids were created by cutting spheres of radii 4–6 Å and removing 8, 16, 32 and 64 Si atoms. The interface Si dangling bonds were then passivated with hydrogen.

Another set of models was generated by introducing unbonded H into the system, and letting the system freely evolve. These H atoms are mobile, and are introduced to study how the network evolves with moving H. This method is unbiased as the H is free to explore the network, form and break bonds as the chemistry and dynamics dictates. Thus, we find that the diffusing H acts as a “strain detector,” being attracted to strained regions, as for example fourfold rings. The models are studied with constant temperature thermal simulation for 300 and 700 K for 4 ps (for 20 000 MD steps with a time step of 0.2 fs). All the results correspond to the Si214 DV and Si152 large void models with and without H.

### III. STATIC PROPERTIES OF VOIDS

To study the structure of the internal surfaces of voids, we have chosen models of (a) DV and (b) large voids. The interface of the void before and after introducing H is compared in both the cases. The results in this section are obtained from a simulation at a constant temperature of 300 K. The proton NMR signatures of voids are also discussed at two different temperatures of 300 and 700 K.

#### A. Structure of unhydrogenated interfaces of voids in *a*-Si

Since the DV and large void models are created from defect-free CRN models, dangling bonds are created only at the void interface. In a DV, there are six dangling bonds at the interface. When the interface is allowed to relax, undercoordinated Si atoms on the interface of the DV bond to leave two dangling bonds. The interface of such a reconstructed DV consists largely of four- and five-member rings. For the interface of a large void with 64 Si atoms removed, 99 Si atoms form the interior surface. There are 24 dangling bonds resulting from the reconstruction along the interface of such a void. The interface atoms form mostly four-, five-, seven-, and eight-member rings. Due to strain at the interface, the bonding is relatively unstable compared to the bulk *a*-Si sites. A dynamical signature of this instability is that interface Si atoms undergo large bond length fluctuations until a diffusing H atom is captured and stabilizes the bonding. An example is shown in Fig. 1.

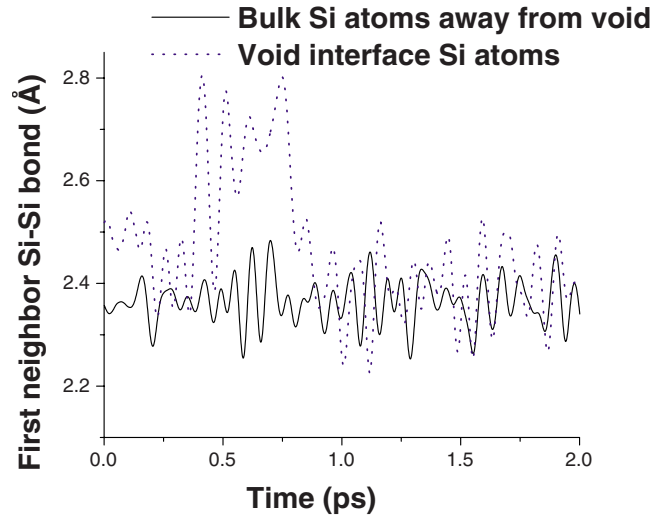


FIG. 1. (Color online) Time-averaged bond fluctuations for Si atoms near divacancy void interface (dotted lines) compared to Si atoms far away from void.

#### B. Structure of hydrogenated interface of voids in *a*-Si:H

To study how H modifies the interface of the voids, we have studied the ring statistics of eight models. Ring statistics for a model with a DV and a large void before and after introducing H is shown in Table I. Ring statistics of CRN models *sans* void is shown for comparison. The model with a DV created from a 64-atom CRN model has more four- and five-member strained rings and fewer six- and seven-member rings. With the introduction of H, a decrease in all rings is observed, as expected, especially the strained four- and five-member rings. A similar phenomenon is observed for a DV generated from the 216 CRN model. For a large void model generated from a 216-atom CRN, there is a significant increase in four-member rings due to strain in the void interface. With introduction of H, there is a remarkable decrease in the number of four- and five-member rings.

#### C. Proton NMR signatures of voids

Recent proton NMR experiments have yielded a frequency spectrum interpreted as arising from dipolar-coupled H pairs separated, on average, by  $1.8 \pm 0.1$  Å. It has been

TABLE I. Ring statistics for various models.

Models	4 #	5 #	6 #	7 #
(Si64 CRN)	0	25	86	177
(Si62 divacancy)	1	28	77	164
(Si62H6)	0	27	70	143
(Si216 CRN)	0	94	176	228
(Si214 divacancy)	6	96	169	224
(Si214H6)	2	89	164	218
(Si152 large void)	15	54	82	124
(Si152H67)	7	50	62	96

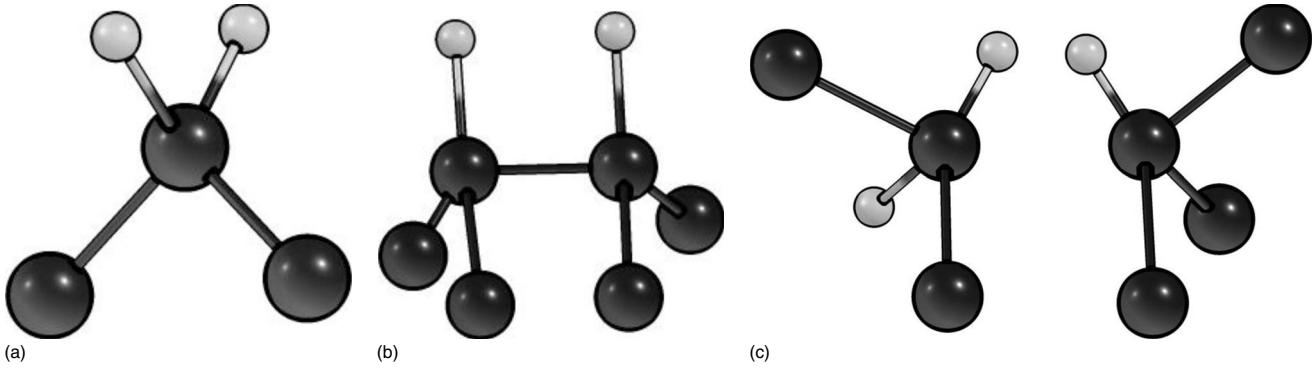


FIG. 2. Conformations of H (a) SiH<sub>2</sub>, (b) H-Si-Si-H, and (c) Si-H H-Si.

further inferred that the responsible microstructure is H clustered in DVs.<sup>16</sup>

In our models with a DV, we computed the distribution of H-H separation and observed a peak at a H-H distance of  $1.8 \pm 0.2$  Å for all the models. Various H configurations exist in the DV models, including the dihydride [Fig. 2(a)] with its characteristic 2.4 Å signature<sup>29</sup> and the Si-H complex where the H atoms are connected to the nearest-neighbor Si atoms [Fig. 2(b)] with a H-H separation of 2.2 Å. A mean H-H distance of 1.8 Å is obtained from two distinct scenarios: H connected to Si atoms that are next-nearest neighbors, -a monohydride (Si-H H-Si) configuration, as shown in Fig. 2(c), and H clustering at the interface of the voids. The void surface comprises either Si-H<sub>2</sub> or Si-H bonding configurations. When unbonded H atoms are introduced and their motion is monitored, it is observed that H tends to form monohydride configurations in pairs with a tendency to cluster along the interface of the void. To illustrate the nature of H clusters at the DV, a representative DV model of *a*-Si:H is shown in Fig. 3. We have studied the temperature dependence of the dynamics of the mobile H atoms and tracked the H-H distance. For both 300 and 700 K, we observed that the mean H-H distance of  $1.8 \pm 0.2$  Å is confirmed for DVs. At 700 K, mobile H atoms are strongly diffusive and all the 6 H atoms cluster around the interface of the voids. At 300 K,

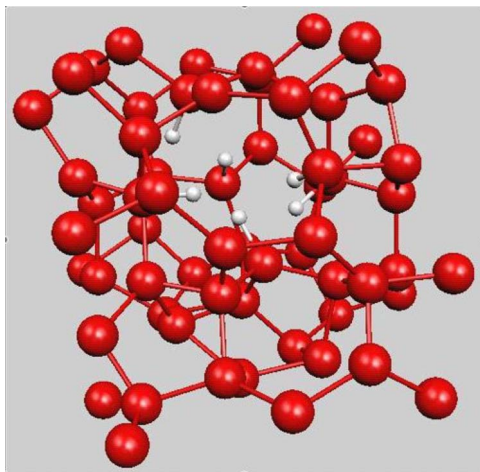


FIG. 3. (Color online) A model of *a*-Si:H with DV showing H clustering around the interface. Small sphere represents H.

although H atoms diffuse toward the strained Si bonds around the void interface and cluster around the interface, a few isolated Si-H bonds are also observed in most cases.

A representative result for the distribution of H-H separation at different temperatures is shown in the Fig. 4. The H-H separation is distributed about 1.88 Å with a full width at half maximum (FWHM) of 0.53 Å which agrees very well with the proton-proton separation extracted from the NMR data by Bobela *et al.*<sup>16</sup> As the figure reveals, the temperature dependence of the H pair distribution function is fairly weak below 400 C.

For a the proton NMR spectrum (assuming homogeneous broadening and a Gaussian line shape from dipolar broadening), the FWHM can be expressed (in kilohertz) as<sup>30</sup>

$$\sigma = 190 \left( \frac{1}{N} \sum_{i,j=1(i \neq j)}^N \frac{1}{r_{ij}^6} \right)^{1/2}, \quad (1)$$

where  $r_{i,j}$  is the distance between nuclei  $i$  and  $j$  in Å, and  $N$  is the total number of spins. We computed  $\sigma$  for 300 and 700 K for a DV model derived from a 216 CRN model.  $\sigma$ (kHz) is found to be 32 kHz at 700 K and 22 kHz at 300 K, which are within the experimental range of 22–33 kHz, attributed to clusters of Si-H.<sup>30</sup> We performed similar studies on the mod-

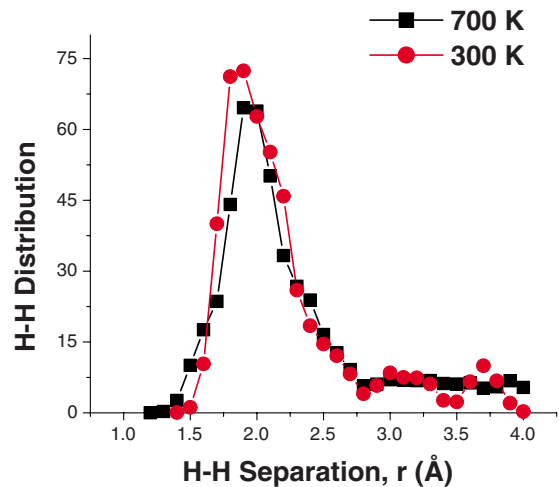


FIG. 4. (Color online) Plot of H-H distribution vs H-H separation. The mean H-H separation is  $\bar{r}=1.88$  Å (1.8 Å) for 700 K (300 K).

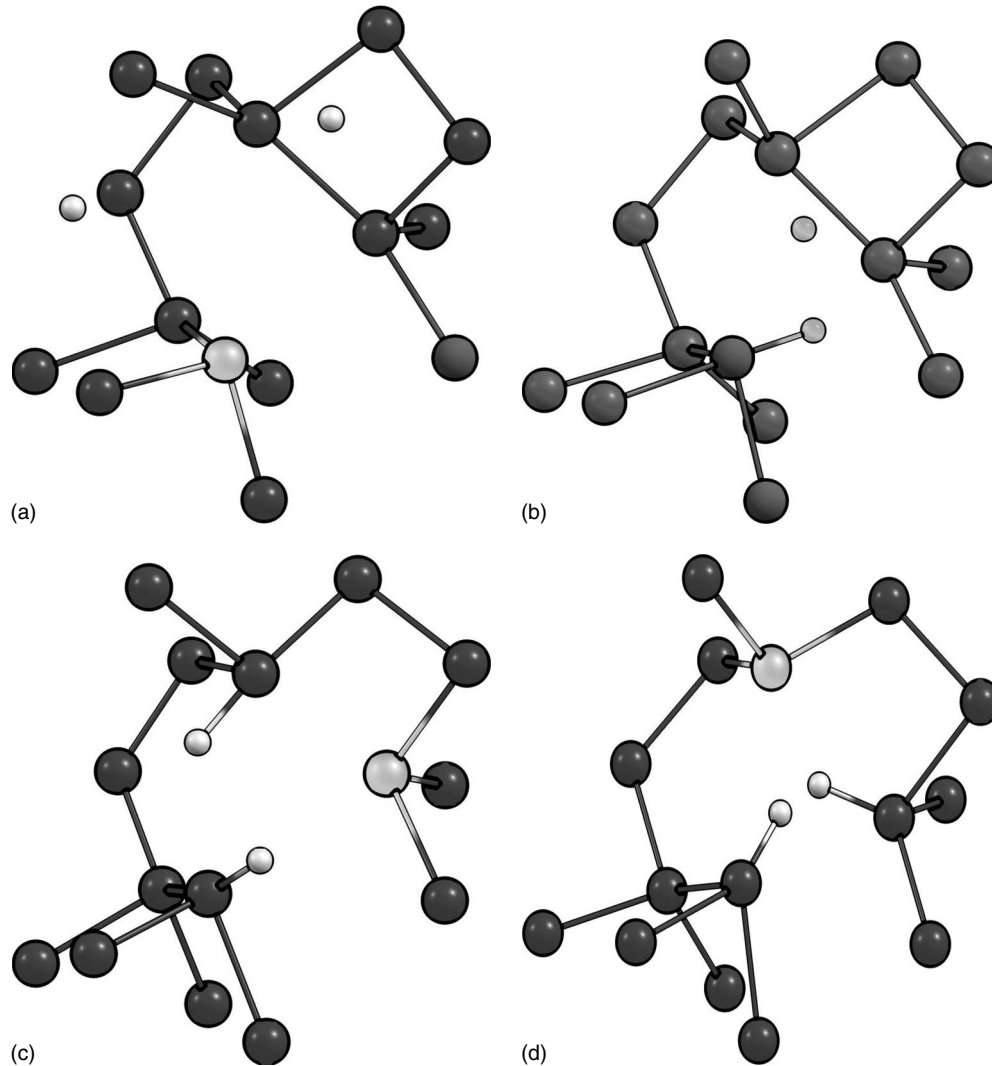


FIG. 5. Role of H in relaxing strain in the network at a particular site in a small divacancy model. H atoms are small light circles, Si atoms are larger and dark, and threefold Si atom is denoted by large light circle. (a) A mobile hydrogen atom approaches a strained four-member ring. (b) One H atom stabilizes a dangling bond and the other approaches bond center of a strained Si-Si bond that is an edge of the ring, (c) H breaks strained Si-Si bond and forms bond with Si, (d) H finally forms SiH-HSi complex and reduces strain.

els with larger voids ( $\text{Si}_{152}\text{H}_{67}$ ). In these models, a H-H separation of  $2.4 \text{ \AA}$  consistently emerges where all complexes are formed. We conclude that the geometric constraints of the DV are such that they promote the experimentally observed H-H separation of  $1.8 \pm 0.1 \text{ \AA}$ , as noted by Bobela *et al.*<sup>16</sup>

#### IV. HYDROGEN DYNAMICS

To study H dynamics for DV and large void models, we tracked the trajectories and bonding statistics of H atoms for a 4 ps MD run at a temperature of 300 K.

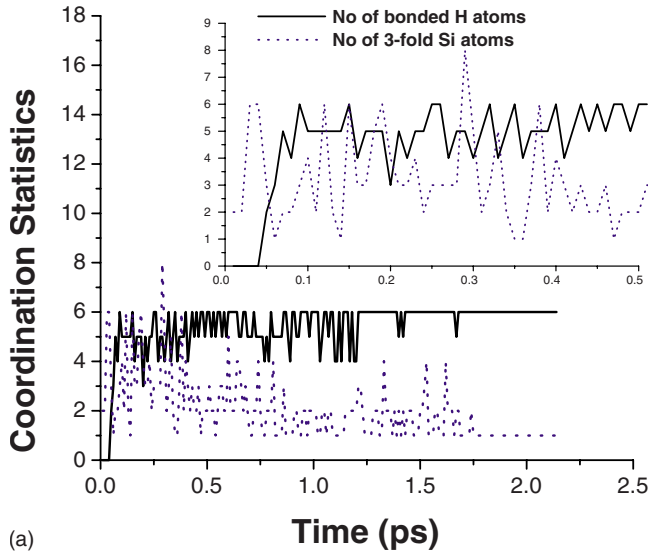
##### A. H mediated reconstruction at the internal surface

We studied reconstruction of the void interfaces in the presence of H. The H atoms play an important role in relaxing the strain in the network, by breaking strained bonds and forming new bonds with either the strained Si atoms or their

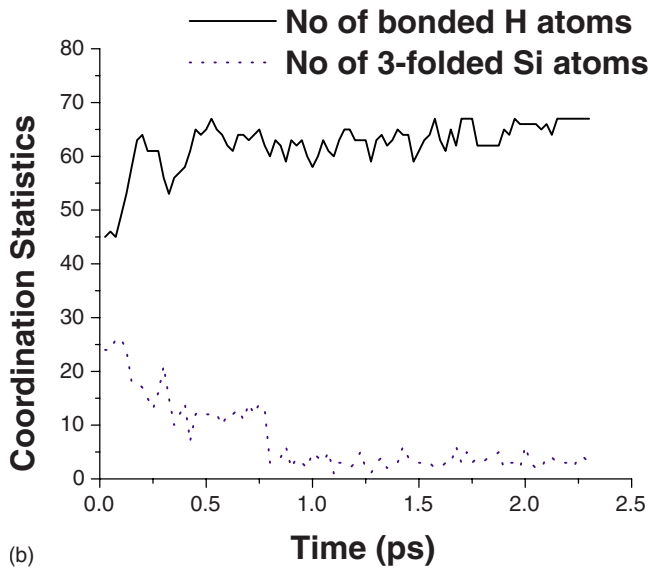
neighbors. To illustrate the role of hydrogen in the surface reconstruction of the void, we have chosen a very strained interface of a DV. The interface includes a four-member ring upon relaxation without H. When mobile hydrogen atoms are introduced into the network, they preferentially attack the strained bonds and finally form Si-H bond and hence eliminate the four-member ring. Snapshots of this phenomenon are shown in Fig. 5. In a larger void also, H atoms play an important role in reducing the number of four-, five- or even seven-, eight-member rings.

##### B. Creation and annihilation of dangling bonds

Mobile H atoms diffuse through the network and play a very active role in forming and breaking bonds.<sup>31</sup> These processes proceed as the H atoms break strained Si bonds resulting from reconstruction of the interface, and finally form Si-H or  $\text{SiH}_2$  complexes. The number of dangling bonds in the system decreases as expected as the H explores the net-



(a)



(b)

FIG. 6. (Color online) Coordination statistics vs time (ps) for (a) a divacancy (early coordination fluctuation is shown in the inset), and (b) large void (see text).

work. The pattern of diffusion depends on the local environment and geometry around the H atoms. In Fig. 6, we report the time dependence of the number of dangling and Si-H bonds for DV and large voids. We have chosen a model with DV ( $\text{Si}_{214}\text{H}_6$ ) atoms. The 6 H atoms are initially unbonded. They quickly form Si-H bonds within ca. 0.1 ps. Consequently, the number of dangling Si bonds first decreases as the H atoms find suitable dangling bonds to passivate. The number of dangling bonds then fluctuates due to an equilibrium involving a chain of bond breaking and bond forming events. Finally, the number of dangling bonds stabilizes after all the H atoms have formed well-bonded Si-H complexes. For the large void model, we have observed similar behavior. However, large numbers of dangling Si bonds are initially present, for example, for a ( $\text{Si}_{152}\text{H}_{67}$ ) model, there are 24 dangling Si bonds to start with. Although significant decrease in the number of dangling bonds is observed, after the end of 4 ps run, there are still four dangling bonds present. There is

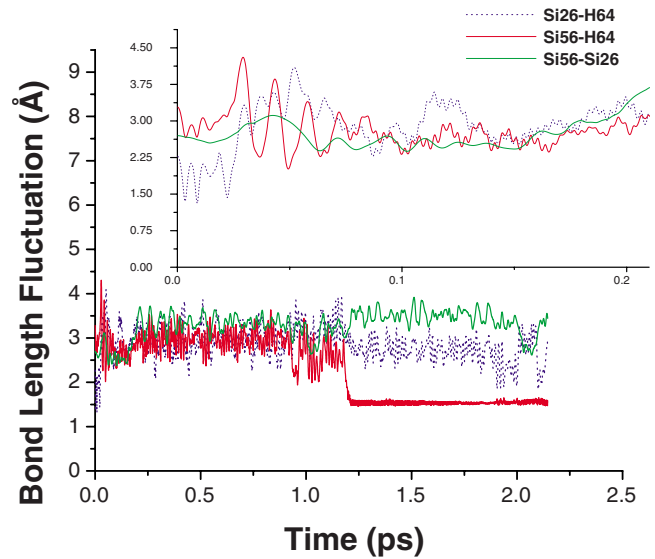


FIG. 7. (Color online) Bond length fluctuation between  $\text{H}_{64}$  and  $\text{Si}_{26}$  and  $\text{Si}_{56}$ , and between  $\text{Si}_{26}$  and  $\text{Si}_{56}$ . Dotted line indicates the bond fluctuation between  $\text{H}_{64}$  and  $\text{Si}_{26}$  which were initially bonded.  $\text{H}_{64}$  breaks bond with  $\text{Si}_{26}$  and hops between  $\text{Si}_{26}$  and  $\text{Si}_{56}$ . Dark solid line plot shows  $\text{H}_{64}$  finally bonds with  $\text{Si}_{56}$ . Light solid line shows  $\text{Si}_{26}$  and  $\text{Si}_{56}$  were bonded initially before  $\text{H}_{64}$  breaks  $\text{Si}_{26}$ - $\text{Si}_{56}$  bond. The initial bond fluctuation is shown in the inset.

an expected correlation between the number of Si-H bonds and the number of dangling Si bonds as seen in Fig. 6.

To further describe void-mediated bond breaking and bond formation, we have tracked one representative diffusing H atom, and the surrounding interface Si atoms with which it forms and breaks bonds.  $\text{H}_{64}$  bonds briefly with  $\text{Si}_{26}$ , and then hops between  $\text{Si}_{26}$  and  $\text{Si}_{56}$  for 1.3 ps and finally forms bonds with  $\text{Si}_{56}$  ( $\text{Si}_{56}$  and  $\text{Si}_{26}$  were neighbors). As a result of fluctuating bond center detachment,<sup>7</sup> the bond between  $\text{Si}_{26}$  and  $\text{Si}_{56}$  breaks. The bond lengths between  $\text{Si}_{26}$ ,  $\text{Si}_{56}$ , and  $\text{H}_{64}$  are plotted to show how H motion influences bonding between interface Si atoms in Fig. 7.

### C. Formation of $\text{H}_2$ molecule

The formation of  $\text{H}_2$  molecule was detected in the case of large voids with excess H content. Although the statistics are very limited and the formation of molecule is observed only in a few cases, we consider the result to be quite interesting and relevant to experimental observations.<sup>14,15</sup> The formation of  $\text{H}_2$  molecule is observed in (a) cases when two diffusive H atoms get sufficiently close ( $\approx 2 \text{ \AA}$ ) (Ref. 35), and (b) when the mobile H atoms come too close to a bonded H atom while diffusing through the network, break Si-H bond, and form a  $\text{H}_2$  molecule. The second case can be seen as a mechanism to create new dangling bonds.  $\text{H}_2$  molecules are seen to form only inside large voids with excess H and they appear to be trapped inside such voids, at least for the few ps time scales that we can easily investigate. The confinement of the  $\text{H}_2$  molecule has been reported experimentally by Borzi *et al.*<sup>32</sup> The trajectories of the H atoms forming the  $\text{H}_2$  molecule are tracked and the H-H distance between  $\text{H}_{192}$  and  $\text{H}_{203}$  forming the molecule is plotted in Fig. 8. As the figure

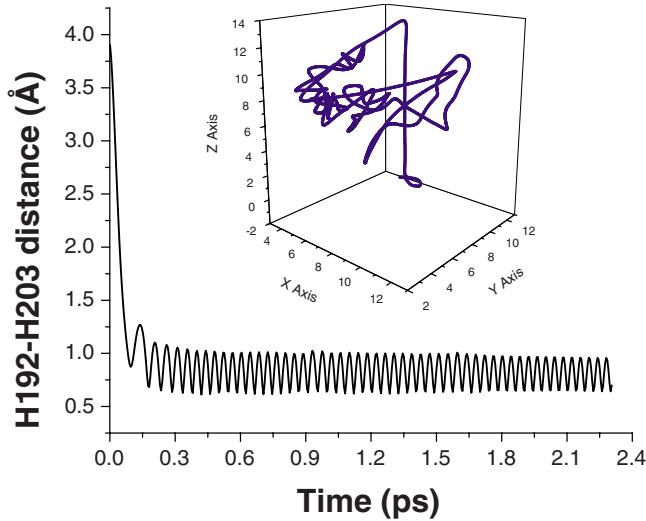


FIG. 8. (Color online) Plot of H-H distance between  $H_{192}$  and  $H_{203}$  showing the formation of the molecule. The trajectory of the two H in the  $H_2$  molecule is shown in the inset. After  $H_2$  formation, motion is confined to the void interior.

reveals, the molecular formation occurs within 0.2 ps and then the H-H distance stabilizes to the value of the molecular bond. The molecule is formed inside the large void. The trajectory of the molecule is shown in the inset of the plot.

## V. ELECTRONIC STRUCTURE

Since the presence of a defect determines the electronic structure, we studied the role of voids on the electronic structure of  $a$ -Si with and without hydrogen.

To study the localization of electronic states, we computed the local charge  $q(n, E)$  for each eigenvalue with energy  $E$  and atomic site  $n$ , and the inverse participation ratio (IPR):

$$\text{IPR} = \sum_n q(n, E)^2, \quad (2)$$

and the electronic density of states (EDOS) for models with voids before and after introducing H. For an ideally localized state where all the charges are localized on a single atomic site,  $\text{IPR} = 1$ . For uniformly extended states,  $\text{IPR} = 1/n$ . Thus, IPR is a measure of localization. For each eigenvector, we determine the atoms where the charges are the most localized. The intent is to study the correlation between localized states and the local topology for the atoms where the charge is largest. This represents an attempt to understand the connection between chemical reactivity and electron localization in  $a$ -Si:H.

For both DV and large voids, localized states reside on the interface Si atoms which have dangling bonds or highly strained bonds associated with them. The most localized eigenstates are at the top of the valence band [highest occupied molecular orbital (HOMO) level] and the bottom of the conduction band [lowest unoccupied molecular orbital (LUMO) level], and these states form filamentary structures, as detected in earlier reports for  $a$ -Si.<sup>2,33,34</sup> The filaments

begin at the surface of the voids and extend into the bulk. In these filamentary structures, the most localized atoms in the HOMO states are connected with short bonds (average 2.2 Å) and with shorter bond angles and the most localized atoms in the LUMO states are connected with longer bond length (average 2.7 Å) and broader bond angles as reported earlier.<sup>2,33,34</sup>

In the case of  $a$ -Si:H, H atoms either terminate the dangling Si bonds or break strained Si-Si bonds to form Si-H complexes. In the DV models, about 66% of the H atoms are bonded to the most localized Si atoms. In case of large void models, about 80% of the H atoms are bonded to the most localized Si atoms (meaning those atoms contributing to strongly localized states). After hydrogenation the filaments persist. To elucidate the filamentary structure, the most localized atoms (40% of charge) are denoted by black (red online), the lesser localized atoms (20–25% of charge) are denoted by gray (gold online), and the even less localized atoms (5% charge) by white (yellow online) such that 65–70% of total charge localization is shown in Fig. 9. Figures 9(a) and 9(b) show the two filamentary structures of the localized atoms in the HOMO and LUMO state for a DV. Figure 9(c) is representative of the localized state in the HOMO state in a large void.

To compare the degree of localization of the localized states, the IPR after introducing H is plotted in Fig. 10 for DV and large void models of  $a$ -Si:H with the Fermi level shifted to zero. The vertical bars in the IPR plot reveal the extent of localization (taller bars, higher localization). The EDOS before and after introducing H for a DV and large void models are also plotted in Fig. 10. For a DV, without the introduction of H, the EDOS shows a gap. With the introduction of H, the defect density decreases as H passivates the dangling bonds. This results in the further opening of the gap as seen for a DV in Fig. 10(a). The IPR for a DV model of  $a$ -Si:H shows well localized states in the tail states around the Fermi level. For large void system without H, the EDOS has a large number of defect states in the gap. With the introduction of H, a decrease in the defect density and mid-gap states is observed. Figure 10(b) illustrates how the introduction of H reduces the defect states for the case of the  $\text{Si}_{152}\text{H}_{67}$  model. However, there are still a few midgap states present. As discussed in Sec. IV B, for this model, four dangling bonds exist after the 4 ps MD run. The IPR for the large void model in  $a$ -Si:H clearly shows that the midgap states in the EDOS are constituted of four localized states. Longer simulation time might well help in further dangling bonds and hence the midgap states appearing in the EDOS. In any event it is clear that H plays an important role in reducing the defect densities in the void interfaces.

## VI. CONCLUSIONS

We have studied the dynamics of H in  $a$ -Si:H with various voids and H concentration by using *ab initio* techniques. Representative trajectories of diffusive mobile hydrogen atoms are tracked and the resulting bonding configurations are reported. Our results help to confirm the interpretation of recent NMR experiments.<sup>16</sup> For models with unbonded hy-

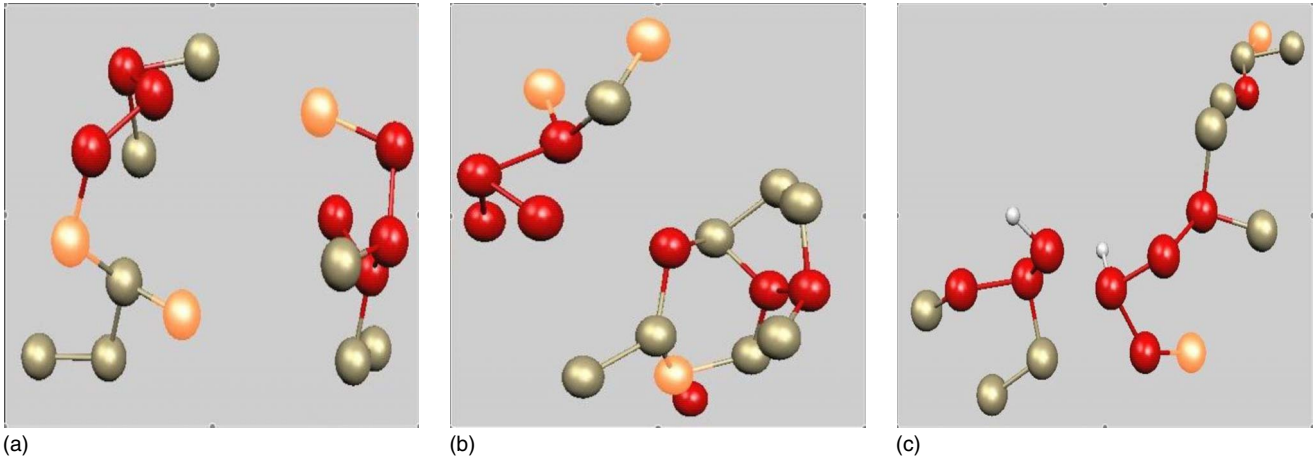


FIG. 9. (Color online) Atoms with highest charge localization and filamentary structures for (a) HOMO state in a divacancy, (b) LUMO state in a divacancy, and (c) HOMO state in a large void. H atoms (small spheres) attached to the most localized Si atoms in the HOMO state of a large void are shown. In grayscale, the ordering in descending charge is black, gray, white; in color the ordering in descending charge is red, gold, yellow (see text).

drogen, it is observed that hydrogen tends to form monohydride configurations in pairs, an indication of hydrogen clustering. H clustering around the interface of DV gives rise to an H-H separation of  $1.8 \pm 0.1$  Å. In cases of large void, the

H-H separation is found to be 2.4 Å. In these large voids, with excess H content, formation of H<sub>2</sub> molecules inside the voids is also seen. Our results show that H plays an important role in reducing the number of rings and dangling bonds

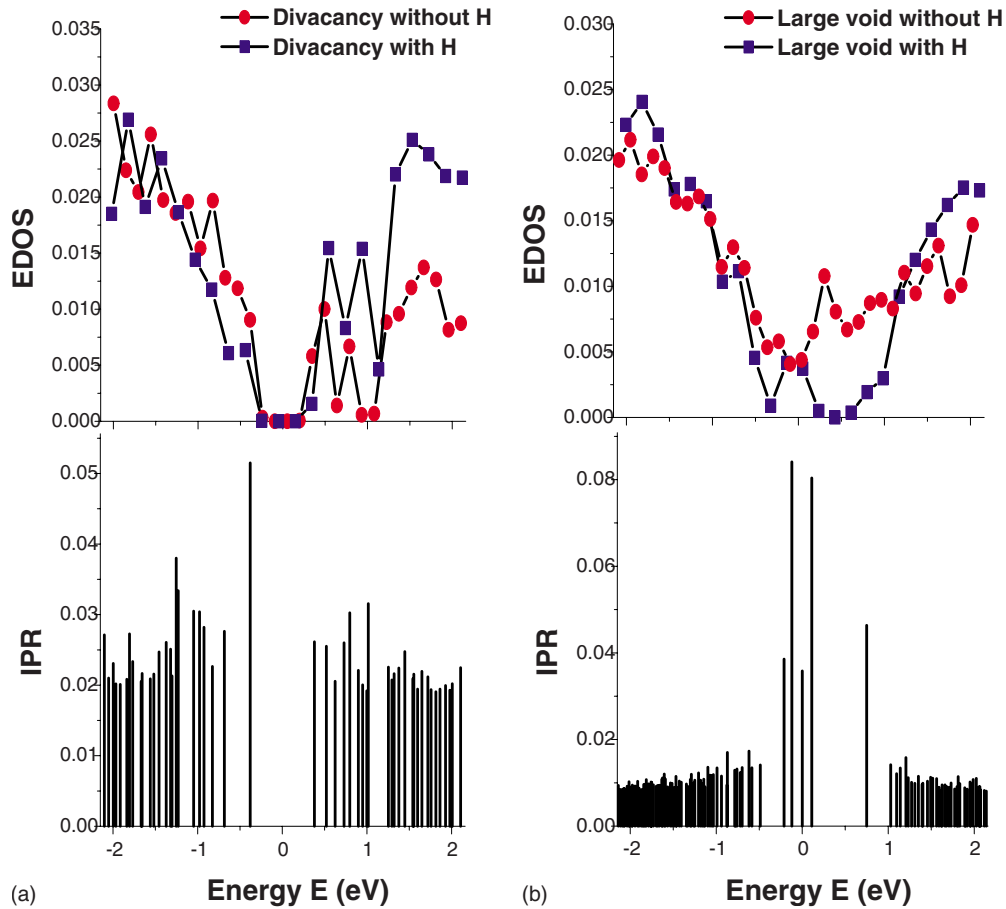


FIG. 10. (Color online) Plots of electron localization gauged by IPR (see text) after introducing H and state density (EDOS) vs the energy before and after introducing H for the (a) divacancy void and (b) large void with 64 Si atoms removed. The Fermi level is shifted to zero. The lines decorated with solid circles are the EDOS before introducing H for a divacancy and large void model. The lines with solid squares are the EDOS after introducing H.

at the interfaces of the voids. H is found to be highly reactive with strained parts of the network, and thus reacts strongly with voids.

#### ACKNOWLEDGMENTS

This research was sponsored by the U.S. Army Research Office and U.S. Army Research Laboratory and was accomplished under Cooperative Agreement No. W911NF-0-2-

0026. We gratefully acknowledge the National Science Foundation for support under Grant No. DMR-0605890. D.A.D. thanks the Leverhulme Trust (U.K.) and the NSF International Materials Institute for New Functionalities in Glass under Grant No. DMR-0409588 for supporting work undertaken at the University of Cambridge. We thank J. R. Abelson, P. M. Voyles, D. C. Bobela, and P. C. Taylor for many discussions. D.A.D. thanks S. R. Elliott for hospitality at Trinity College, Cambridge.

- 
- <sup>1</sup>J. Dong and D. A. Drabold, Phys. Rev. Lett. **80**, 1928 (1998).  
<sup>2</sup>J. J. Ludlam, S. N. Taraskin, S. R. Elliott, and D. A. Drabold, J. Phys.: Condens. Matter **17**, L321 (2005).  
<sup>3</sup>T. A. Abteu, M. Zhang, and D. A. Drabold, Phys. Rev. B **76**, 045212 (2007).  
<sup>4</sup>P. B. Allen and J. L. Feldman, Phys. Rev. Lett. **62**, 645 (1989).  
<sup>5</sup>P. M. Voyles, Ph.D. thesis, University of Illinois at Urbana-Champaign, 2001; P. M. Voyles and J. R. Abelson, Sol. Energy Mater. Sol. Cells **78**, 85 (2003); S. M. Nakhmanson, P. M. Voyles, N. Mousseau, G. T. Barkema, and D. A. Drabold, Phys. Rev. B **63**, 235207 (2001).  
<sup>6</sup>S. M. Nakhmanson and D. A. Drabold, Phys. Rev. B **58**, 15325 (1998); **61**, 5376 (2000).  
<sup>7</sup>T. A. Abteu, F. Inam, and D. A. Drabold, Europhys. Lett. **79**, 36001 (2007).  
<sup>8</sup>R. A. Street, *Hydrogenated Amorphous Silicon* (Cambridge University Press, Cambridge, UK, 1991).  
<sup>9</sup>Peter D'Antonio and John H. Konnert, Phys. Rev. Lett. **43**, 1161 (1979).  
<sup>10</sup>David L. Young, Paul Stradins, Yueqin Xu, Lynn M. Gedvilas, Eugene Iwaniczko, Yanfa Yan, Howard M. Branz, Qi Wang, and Don. L. Williamson, Appl. Phys. Lett. **90**, 081923 (2007).  
<sup>11</sup>W. E. Carlos and P. C. Taylor, Phys. Rev. B **26**, 3605 (1982).  
<sup>12</sup>J. Baum, K. K. Gleason, A. Pines, A. N. Garroway, and J. A. Reimer, Phys. Rev. Lett. **56**, 1377 (1986).  
<sup>13</sup>C. Longeaud, J. Optoelectron. Adv. Mater. **4**, 461 (2002).  
<sup>14</sup>W. Beyer, Physica B **170**, 105 (1991).  
<sup>15</sup>P. Roura, J. Farjas, C. Rath, J. Serra-Mirallas, E. Bertran, and P. Roca i Cabarrocas, Phys. Rev. B **73**, 085203 (2006).  
<sup>16</sup>D. C. Bobela, T. Su, P. C. Taylor, and G. Ganguly, J. Non-Cryst. Solids **352**, 1041 (2006).  
<sup>17</sup>K. A. Kilian, D. A. Drabold, and J. B. Adams, Phys. Rev. B **48**, 17393 (1993).  
<sup>18</sup>P. Ordejón, E. Artacho, and J. M. Soler, Phys. Rev. B **53**, R10441 (1996).  
<sup>19</sup>D. Sanchez-Portal, P. Ordejón, E. Artacho, and J. M. Soler, Int. J. Quantum Chem. **65**, 453 (1997).  
<sup>20</sup>J. M. Soler, E. Artacho, J. D. Gale, A. Garcia, J. Junquera, P. Ordejón, and D. Sanchez-Portal, J. Phys.: Condens. Matter **14**, 2745 (2002).  
<sup>21</sup>N. Troullier and J. L. Martins, Phys. Rev. B **43**, 1993 (1991).  
<sup>22</sup>L. Kleinman and D. M. Bylander, Phys. Rev. Lett. **48**, 1425 (1982).  
<sup>23</sup>J. P. Perdew, K. Burke, and M. Ernzerhof, Phys. Rev. Lett. **77**, 3865 (1996).  
<sup>24</sup>C. G. Van de Walle, Phys. Rev. B **49**, 4579 (1994).  
<sup>25</sup>R. Atta-Fynn, P. Biswas, P. Ordejón, and D. A. Drabold, Phys. Rev. B **69**, 085207 (2004).  
<sup>26</sup>G. Kresse and J. Furthmüller, Comput. Mater. Sci. **6**, 15 (1996); Phys. Rev. B **54**, 11169 (1996).  
<sup>27</sup>G. T. Barkema and Normand Mousseau, Phys. Rev. B **62**, 4985 (2000).  
<sup>28</sup>F. Wooten, K. Winer, and D. Weaire, Phys. Rev. Lett. **54**, 1392 (1985).  
<sup>29</sup>T. A. Abteu, D. A. Drabold, and P. C. Taylor, Appl. Phys. Lett. **86**, 241916 (2005).  
<sup>30</sup>Y. Wu, J. T. Stephen, D. X. Han, J. M. Rutland, R. S. Crandall, and A. H. Mahan, Phys. Rev. Lett. **77**, 2049 (1996).  
<sup>31</sup>P. Biswas, D. N. Tafen, F. Inam, B. Cai, and D. A. Drabold, J. Phys.: Condens. Matter **21**, 084207 (2009), especially §7.  
<sup>32</sup>R. Borzi, P. A. Fedders, P. H. Chan, J. Herberg, D. J. Leopold, and R. E. Norberg, J. Non-Cryst. Solids **299-302**, 205 (2002).  
<sup>33</sup>P. A. Fedders and D. A. Drabold, Phys. Rev. B **47**, 13277 (1993); P. A. Fedders, D. A. Drabold, and S. Nakhmanson, *ibid.* **58**, 15624 (1998).  
<sup>34</sup>Y. Pan, F. Inam, M. Zhang, and D. A. Drabold, Phys. Rev. Lett. **100**, 206403 (2008); Y. Pan, M. Zhang, and D. A. Drabold, J. Non-Cryst. Solids **354**, 3480 (2008).  
<sup>35</sup>Obviously, for a full treatment, the molecular formation probability depends upon the atomic velocities and environment.